Progress In Electromagnetics Research, PIER 87, 197–214, 2008

RESONANCE SPLITTING IN TWO COUPLED CIRCULAR CLOSED-LOOP ARRAYS AND INVESTIGATION OF ANALOGY TO TRAVELING-WAVE OPTICAL RESONATORS

I. Psarros and I. Chremmos

School of Electrical and Computer Engineering
National Technical University of Athens
9 Iroon Polytechniou Str., Zografos 15780, Athens, Greece

Abstract—A well known property of large circular closed-loop arrays is that when the dimensions and the distance of the cylindrical dipoles are properly chosen, the arrays possess very narrow resonances. As far as single isolated loop arrays are concerned, the phenomenon has been predicted and analyzed in the past in the framework of "two-term" theory. In the present paper the same methodology is, for the first time, applied to investigate the system of two coupled identical circular arrays. It is found that the spectral profile of this new array is characterized by the coupling-induced splitting of the resonances of the single loop array into symmetric and antisymmetric supermodes, in direct analogy with other types of coupled electromagnetic cavities. Due to the circular symmetry of the individual arrays, the phenomenon is strongly correlated to the optical counterpart of two coupled traveling-wave optical resonators, such as whispering gallery or microring resonators. By borrowing the resonance splitting model from optical resonators, this analogy connection is investigated and interesting conclusions are reached.

1. INTRODUCTION

It is the result of theoretical and experimental research [1–12] that large circular arrays (consisting of many elements N and having a circumference of many wavelengths) of identical, parallel and non-staggered cylindrical dipoles possess a series of very narrow resonances, when the inter-element spacing d, the length and the radii of the identical dipoles are properly selected. Resonance means that the driving-point conductance has a maximum with a very large value,

while the driving-point susceptance is zero. A series of narrow resonances occur as the electrical length of the dipoles is varied. This has been observed experimentally in [3, 5] and theoretically in [1], where the varying parameter is the frequency. In [1] only a single element is driven and a particular phase sequence m ($m = N/2, N/2-1, \ldots$), is associated with each resonance. Resonances with larger m occur at higher frequencies. For higher frequencies the resonances are narrower. The narrowest resonance corresponds to the maximum value of m which is equal to $N/2$ (or to $(N-1)/2$ if N is odd). When resonance occurs, the currents on all N elements are large. The distribution of the currents around the array can be thought of as a slow standing wave which can be described by $\cos\left[\frac{2\pi(l-1)m}{N}\right], l = 1, 2, \ldots, N$ [2, 4, 10]. The circumference C of the array is always an integer multiple of the effective wavelength λ_m of the wave that is supported by the array [9, 10], i.e., $C = |m|\,\lambda_m$.

The resonant properties of circular closed-loop arrays are evidence of their behavior as electromagnetic cavities oscillating with resonant modes which are guided around the circumference thanks to the coupling mechanism between the radiating dipole elements. In the field of optics, similar resonant modes are trapped in dielectric microdisks and propagate very close to their boundary by continuous total internal reflections. Due to the analogy of this mechanism with the classical problem of acoustic propagation along concave surfaces [13], these optical cavities have been termed "whispering gallery" (WG) resonators [14] and constitute a deeply studied type of resonator with extensive applications [15, 16]. Similar properties are exhibited by circular microring resonators which replace disks when resonances of higher-radial order are unwanted and behave as bent dielectric waveguides. Both types of resonators can be referred to with the established term "traveling-wave" (TW) — in contrast to the standing-wave-resonators. Similarly to circular dipole arrays, modes supported by TW resonators are also based on a constructive self-interference condition which is that the round-trip phase acquired by the trapped wave on resonance is an integer multiple of 2π. The resonances are manifested as narrow peaks in the transmitted or reflected power spectrum, which are obtained when these cavities are coupled to external waveguides in order to realize wavelength-selective filters [17].

The complexity of the resonance problem increases when two electromagnetic cavities are coupled together. In TW optical resonators, the case has already been studied [18] as the fundamental representative of a currently attractive class of super-resonators termed "photonic molecules", which includes cluster architectures of coupled resonators [19]. The filter application of the double-microring system

has also been proposed for the implementation of tunable optical reflectors [20, 21]. The coupling of resonators causes the splitting of their individual modes to bonding (symmetric) and antibonding (antisymmetric) supermodes, which are characterized, respectively, by even or odd parity with respect to the symmetry plane, and the frequency splitting is proportional to the inter-resonator coupling coefficient.

Based on the outlined analogy between circular arrays and cylindrical dielectric resonators, it follows that the study of coupling between two identical circular arrays would normally be the next step, leading to the analysis and implementation of more complex, super-resonator configurations of coupled closed-loop arrays. In this paper, for the first time to the authors' knowledge, the "two-term" theory is applied to investigate the resonant properties of a coupled pair of identical circular arrays of dipoles. The numerical results confirm the expected splitting of the resonances of the isolated array to neighbor resonances, which correspond to coupled supermodes with symmetric or antisymmetric dipole current distributions along the arrays, with respect to the symmetry plane. The frequency splitting is found to be a decreasing function of the minimum distance between the arrays. The equivalence between the RF structure and its optical counterparts is further explored by seeking a connection of the magnitude of frequency splitting with the inter-dipole coefficients of mutual coupling predicted by the "two term" theory, in analogy to the corresponding familiar formula connecting frequency splitting and coupling coefficient in TW resonator pairs.

2. TWO-TERM THEORY MODELING OF TWO COUPLED CIRCULAR CLOSED-LOOP ARRAYS

The geometry of two coupled identical circular arrays with N elements each is shown in Fig. 1. We choose to excite only one of the dipoles,

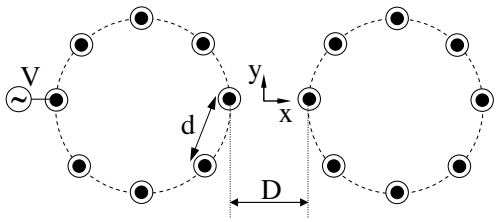

Figure 1. Geometry of two coupled circular dipole arrays with one voltage-driven dipole.

the one on the azimuthal position $\theta = 180°$ in the left array, so that only symmetrical modes with respect to the x-axis are excited on the coupled system (N is assumed to be even). From the problem of the single array [1–5], it is known that, for resonances to occur, one must properly select the inter-element spacing d, as well as the dipoles' length $2h$ and radius a.

Dipole arrays can be effectively analyzed by the semi-analytical approach of "two-term" theory, originally developed by R. W. P. King (see [4] for original references). The method is based on an approximate solution to the N coupled integral equations for the currents of N mutually coupled dipoles, under the hypothesis that each current can be expressed as the sum of two terms. The usual $\sin(k(h-|z|))$ term, as well as the "shifted cosine" term $\cos(kz)-\cos(kh)$, where $k=\omega/c$, h is the half-length of each dipole, a is its radius and the dipoles are z-directed. The coefficients of $\sin(k(h-|z|))$ are given by closed-form, explicit expressions computable via numerical integrations, whereas the N coefficients of the shifted cosine are found by solving a $N\times N$ system of linear algebraic equations. Assuming that $kh \neq \pi/2$, the currents are

$$I_n(z) = \frac{j2\pi}{\zeta_0 \psi_{dR} \cos kh} \left[V_n \sin k\left(h-|z|\right) + t_n\left(\cos kz - \cos kh\right)\right], \quad n = 1,\ldots,N \qquad (1)$$

where V_n is the voltage applied to element n, $\zeta_0 = \sqrt{\mu_0/\varepsilon_0} = 376.73\,\text{ohms}$, ψ_{dR} is a simple integral containing h and a, and the coefficients t_n are determined by solving the $N\times N$ system of linear algebraic equations

$$\sum_{\ell=1}^{N} D_{n\ell} t_\ell = \sum_{\ell=1}^{N} P_{n\ell} V_\ell, \quad 1 \le n \le N \qquad (2)$$

This system can be written in matrix form as $[D]\{t\} = [P]\{V\}$ where the components of the matrices D and P depend on the characteristics of the dipoles (length and radius) and on the inter-dipole distance [4].

For our numerical experiments, we consider perfectly conducting dipoles with length $2h = 1.42$ and radius $a = 0.058$ and circular arrays consisting of $N = 72$ elements arranged around a circle with radius $R = 11.46$, which gives an inter-element spacing $d = 2R\sin(\pi/\mathrm{N}) = 1$. The length unit for dimensions and wavelength is chosen arbitrarily (scaling property of Maxwell equations). To use as a reference, we have initially applied the "two-term" theory method to a single isolated array. Fig. 2 shows the computed driving-point conductance G over the wide wavelength window $3.335 < \lambda < 3.6$. The diagram is characterized

by a set of distinct sharp peaks corresponding to the resonances (free-space wavelength λ_m) of the circular array with an azimuthal order that increases with decreasing wavelength. These resonances have been well studied both theoretically and experimentally in previous works [1–12].

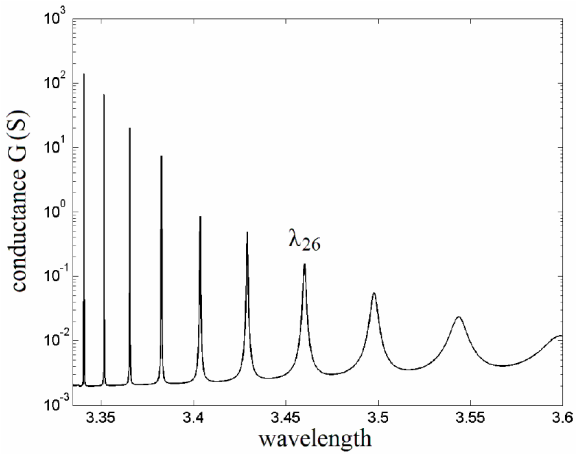

Figure 2. Driving-point conductance G versus wavelength for an isolated circular array with the parameters $N = 72$, $2h = 1.42$, $a = 0.058$, $d = 1.0$. The length unit is arbitrary.

We have subsequently built the linear system (2) of "two-term" theory for two coupled arrays (Fig. 1) at a minimum distance $D = 0.75$ and by assuming the symmetrical voltage excitation mentioned before. Fig. 3 shows the computed driving-point conductance G over the wavelength window $3.35 < \lambda < 3.55$, in comparison to the single array case of Fig. 2. It is clear that each resonance of the isolated array is now split into two lying close and on either side of its initial position. These are clearly the split resonances which are observed in any system of coupled resonant cavities and correspond to symmetric and antisymmetric coupled states (supermodes) with respect to the middle plane of symmetry. Because of its smoother field variation between the coupled cavities, the lower resonance (larger wavelength) is always the symmetric (even) one, while the higher resonance (smaller wavelength) is the antisymmetric (odd) one which has a field node exactly on the plane of symmetry. In other words, in an arbitrary m-th order resonance, we should have $\lambda_m^o < \lambda_m < \lambda_m^e$, where λ_m^e, λ_m^o are respectively the resonant wavelengths of the even and odd supermode.

The picture of supermodes with even and odd field patterns is verified in our "discrete" system through the computation of the $2N$

dipole currents exactly on the split resonances. Fig. 4 shows the amplitude ratio and phase difference between the computed complex currents of elements which are symmetrically positioned with respect to the symmetry plane $x = 0$, at the lower ($\lambda_{26}^{e} = 3.469$) and higher ($\lambda_{26}^{o} = 3.443$) split $m = 26$ resonance for a minimum distance $D = 0.75$ between the two arrays. As expected, the symmetrically positioned dipoles have, with some tolerance, very close amplitudes and oscillate with phase difference close to 0 or π (see the computed average values in Fig. 4), which confirms the nature and identification of even and odd split resonances in the coupled system.

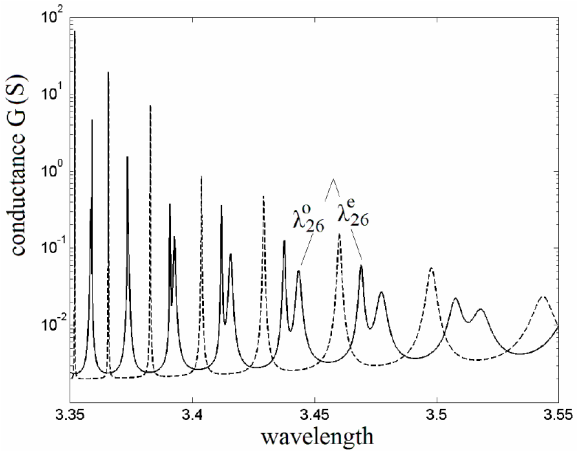

Figure 3. Driving-point conductance G versus wavelength for two coupled identical circular arrays with the parameters of Fig. 2, at a minimum distance $D = 0.75$. The split $m = 26$ even, odd resonances are shown. The dashed line is the conductance of an isolated array.

Figure 5(a) shows the effect of varying the distance between the arrays on resonance splitting by focusing on a wavelength window containing the $m = 26$ resonance. As expected for any system of coupled resonators, it is evident that the splitting of resonances becomes larger as the two arrays approach each other, with the odd and even supermode moving, respectively, to a shorter and longer resonant wavelength due to the need for a faster or slower, respectively, space variation of the field pattern in the coupling region between the two arrays. The dependence of the resonant wavelengths versus the minimum distance are given in Fig. 5(b) where it is noted that the detuning of the split supermodes from the resonance of the single array is not equal.

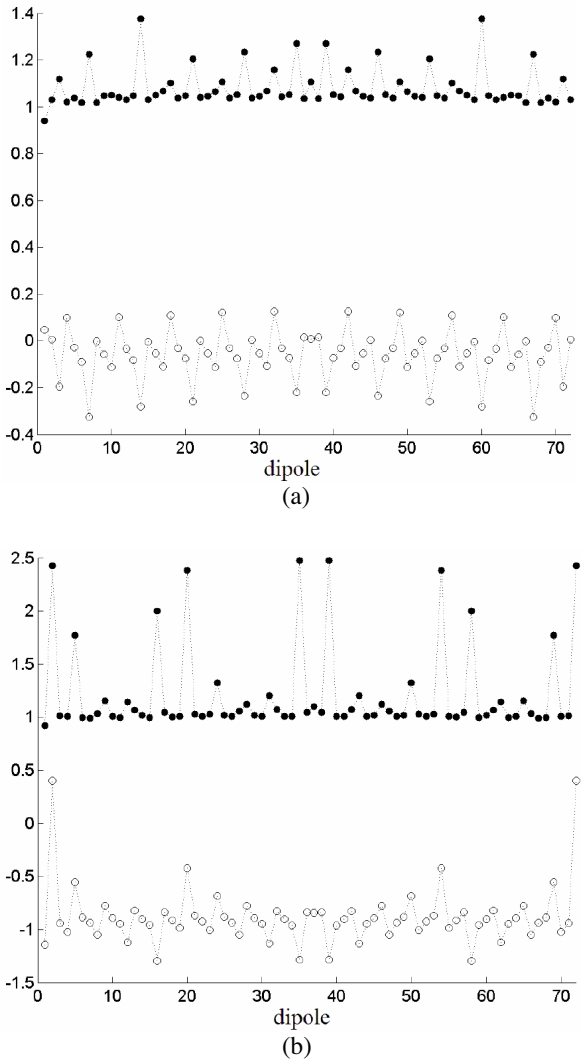

Figure 4. Amplitude ratio (dots) and phase difference — divided by π — (circles) between currents of symmetrically positioned dipoles, with respect to the symmetry plane $x = 0$, in two coupled arrays with $D = 0.75$ at the lower ($\lambda_{26}^{e} = 3.469$) (a) and higher ($\lambda_{26}^{o} = 3.443$), (b) $m = 26$ split resonance. The average amplitude ration is 1.08 (a) and 1.21 (b) and the average phase difference is -0.06π (a) and -0.88π (b).

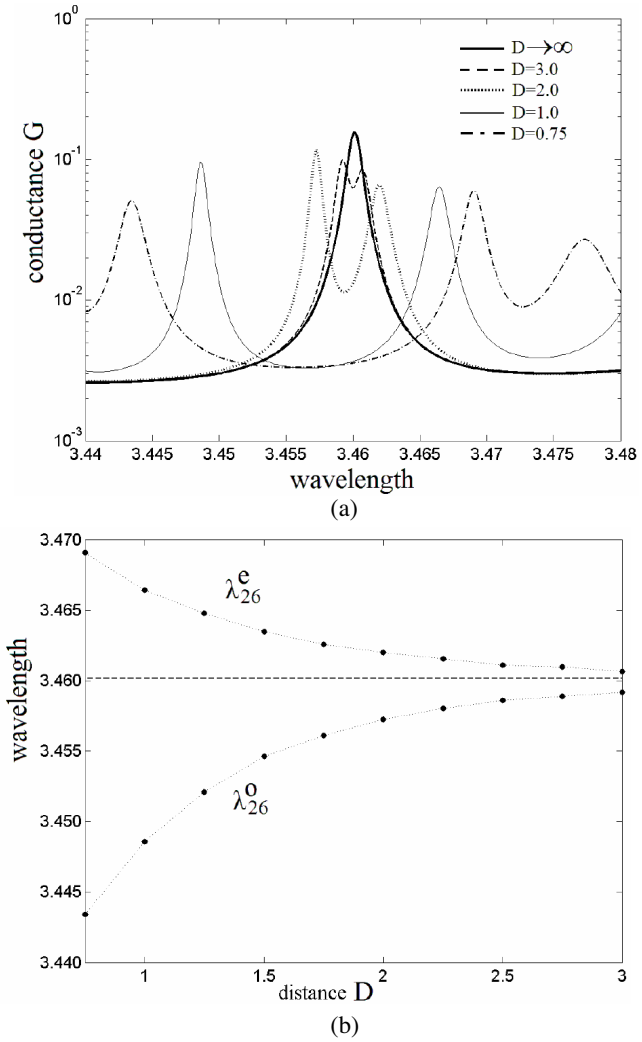

Figure 5. (a) Driving-point conductance G versus wavelength in the vicinity of the $m = 26$ split resonance ($\lambda_{26} = 3.460$) for two coupled identical circular arrays with the parameters of Fig. 2 at different minimum distances D. (b) Resonant wavelengths λ_{26}^{e}, λ_{26}^{o} versus D. The dashed horizontal line is the resonant wavelength λ_{26} for isolated arrays ($D \to \infty$).

3. THE OPTICAL COUNTERPART: COUPLED TW RESONATORS

Owing to the cylindrical symmetry, the modes in an isolated TW optical resonator are double-degenerate with a $\sin / \cos(m\theta)$ azimuthal

field variation. This degeneracy is removed when two identical resonators are brought close together and four non-degenerate coupled modes (supermodes) appear, resulting from the even or odd field symmetry with respect to the two symmetry axes x, y of the structure. We will denote these symmetries as $e_{x,y}$ and $o_{x,y}$. The pairs ($e_x e_y$, $o_x e_y$) and ($e_x o_y$, $o_x o_y$) of the supermodes with the same symmetry with respect to the y axis are nearly degenerate with resonant frequencies that can hardly be distinguished and are called bonding and antibonding supermodes, respectively. The bonding and antibonding supermodes of a coupled pair of resonators are manifested as split resonances of the isolated resonators with a frequency splitting that is proportional to the coupling strength.

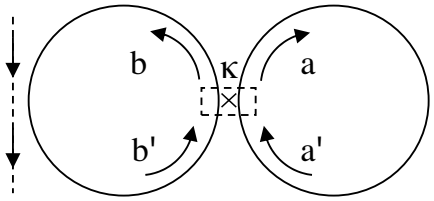

Figure 6. Wave coupling in two coupled TW optical resonators. The vertical dashed line shows the usual way to excite the system through a bus waveguide.

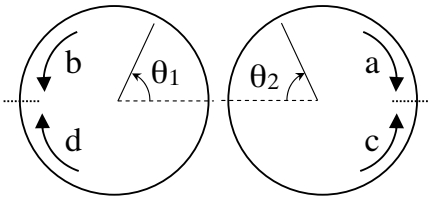

Figure 7. Superposition of counter-propagating waves for the formation of supermodes in two coupled TW optical resonators.

Figure 6 shows the simple standard model that is usually used to explain the mode splitting in coupled TW optical resonators. The coupling of waves is considered to exist only along an infinitesimally long part of the coupling region and is expressed through the matrix equation

$$\begin{pmatrix} a \\ b \end{pmatrix} = \begin{pmatrix} \tau & -j\kappa \\ -j\kappa & \tau \end{pmatrix} \begin{pmatrix} a' \\ b' \end{pmatrix} \tag{3}$$

where a, b and a', b' are the complex field amplitudes of the waves emerging from and entering the coupling region and $\tau(\omega)$, $\kappa(\omega)$ are frequency dependent self- and cross-coupling coefficients which are real for phased-matched coupling and satisfy $\tau^2 + \kappa^2 = 1$ for negligible losses. The propagation around the resonators is expressed by a phase shift ϕ, i.e., $a' = ae^{-j\phi}$ and $b' = be^{-j\phi}$, which is called the round-trip phase and is defined by $\phi = \beta 2\pi R = \omega n_{eff} 2\pi R/c$, where β is the propagation constant and $n_{eff}(\omega)$ is the effective index of the rotating mode and R the resonator radius. Using the last equations into Eq. (3) it is easy to find the resonant condition for the bonding

($a = b$) and antibonding ($a = -b$) supermodes: $\sin\phi(\omega) = \mp\kappa(\omega)$ or $\phi(\omega) = \phi(\omega_0) \mp \sin^{-1}[\kappa(\omega)]$, where $\phi(\omega_0) = 2m\pi$ is the resonance condition for the isolated resonator. In cases where the variation of n_{eff} and κ with frequency can be neglected — which are usually the cases of weak inter-resonator coupling — this condition reveals the symmetrically split resonant frequencies $f = f_0 \mp \delta f$ where δf is proportional to the coupling coefficient κ. Note that when the system is excited by an adjacent bus waveguide (see Fig. 6) coupled to one resonator with coefficient κ', the resonance condition is modified to $\cos\phi = \tau\left(1+\tau'\right)^2/(4\tau')$ which reduces to $\sin\phi = \mp\kappa$ for $\kappa' \ll 1$.

The supermodes can be expressed as linear combinations of counter-rotating waves under the respective condition, by appropriately choosing the corresponding weights so that the desired symmetry with respect to the axes is met. Note that this approach cannot distinguish the resonant frequencies of the previously mentioned degenerate bonding and antibonding mode doublets, which therefore share the same condition. Referring to Fig. 7, the condition $\sin\phi = -\kappa$ corresponds to the bonding supermodes where $a = b$ and $c = d$. The $e_x e_y$ and $o_x e_y$ bonding supermodes follow from the additional choice $c = a$ and $c = -a$, respectively. Similarly, the condition $\sin\phi = +\kappa$ corresponds to the antibonding modes (o_y) where $a = -b$ and $c = -d$. The $e_x o_y$ and $o_x o_y$ antibonding supermodes follow from the additional choice $c = a$ and $c = -a$, respectively.

We now focus on the field variation of the supermodes with even symmetry with respect to the x axis (e_x), by choosing $a = c = 1/2$ which also normalizes the maximum field amplitude to unity. The total field at an azimuthal position θ in the right resonator is given by

$$E(\theta) = ae^{j(\phi/2-\beta R\theta)} + ce^{-j(\phi/2-\beta R\theta)} = \cos\left[\phi\left(\frac{\theta}{2\pi} - \frac{1}{2}\right)\right] \qquad (4)$$

and is the expression of a standing wave. Eq. (4) holds for the bonding ($e_x e_y$) and the antibonding ($e_x o_y$) supermodes provided that the correct corresponding round-trip phase $\phi = \phi_0 \mp \sin^{-1}(\kappa)$ on resonance is used. The field in the left resonator is obviously symmetric or antisymmetric to that of Eq. (4), while the o_x versions of these supermodes simply have the sine instead of the cosine function in Eq. (4). Note also that, since this simple model does not explicitly define the field exactly at the coupling region, one should keep in mind that Eq. (4) is valid for angles $\varepsilon < \theta < 2\pi - \varepsilon$ where 2ε is a small angle.

Figure 8 shows an example of the field amplitudes of the bonding and antibonding e_x supermodes, where we have deliberately chosen a small azimuthal order $m = 4$ and a large coupling coefficient $\kappa = 0.8$ to exaggerate the difference between the two patterns. It is seen that

the odd supermode varies a little faster than the even one, which is due to the difference between their round-trip phases ($\phi = 2m\pi \pm \delta\phi$).

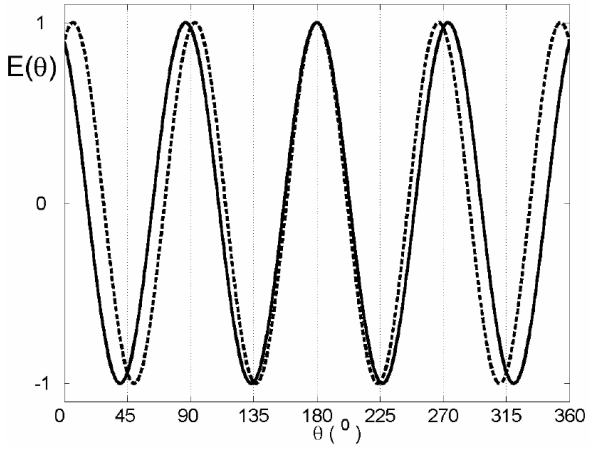

Figure 8. Field amplitude versus azimuth in a TW optical resonator for the $e_x e_y$ bonding (solid line) and the $e_x o_y$ antibonding (dashed line) supermode and the example parameters $m = 4$, $\kappa = 0.8$.

Based on the mentioned analogy between a circular loop array and a TW optical resonator, it is reasonable to expect that the current of the elements of an array in the structure of two coupled arrays will follow a pattern similar to the field pattern in a TW resonator in the structure of two coupled cavities which is given by Eq. (4). In order to investigate this analogy, we will use the dipole currents at the split m-th order resonances of the coupled loop arrays that we have computed in Section 2 using the two-term theory and try to match it with a sampled version of Eq. (4) at the angles θ_i of the elements. The goal is therefore to find the round-trip phase ϕ which minimizes the cost function

$$C(\phi) = \sum_{i=1}^{\mathrm{N}} \left| \hat{E}(\theta_i) - \cos\left[\phi\left(\frac{\theta_i}{2\pi} - \frac{1}{2}\right)\right] \right|^2 \tag{5}$$

where $\hat{E}(\theta_i)$ are the dipole currents normalized by the current of the dipole at $\theta = \pi$, i.e., $\hat{E}(\theta_i) = E(\theta_i)/E(\pi)$. As in the case of mode splitting in optical resonators, the round-trip phases of the closed-loop arrays are expected to satisfy $\phi(\lambda_m^e) < 2m\pi < \phi(\lambda_m^o)$ and their difference will be decreasing with the minimum distance between the two arrays. At infinite distance, the round trip phase of the isolated

array should be exactly $\phi = 2m\pi$ as the current pattern will follow the known formula $\cos(m\theta_i) = \cos(2\pi m \times i/N)$.

Figure 9 shows the variance of cost function $C(\phi)$ at the odd $m = 26$ resonance of the two coupled arrays of Section 1 at a distance $D = 3.0$, occurring at the wavelength $\lambda_{26}^o = 3.459$. There is clearly a very sharp minimum close to the value $\phi \approx 2\pi \times 26$, which justifies our expectations from the previous discussion. The other minima at higher values of ϕ reveal essentially the higher harmonics of the sampled sinusoidal signal $\cos(m\theta_i)$. Indeed, the sequence of currents $\hat{E}(\theta_i)$ can be viewed as a sampling of the signal $\cos(26\theta_i)$ with a rate of 72 samples/period. According to the sampling theorem the sampled signal is composed by an infinite number of harmonics with frequencies $72n \pm 26$ cycles/period (n integer). All harmonics pass from the points $(\theta_i, \hat{E}(\theta_i))$ of the sampled signal and that is the reason why they appear as minima of the cost function. Letting $n = 0,\ 1,\ 2,\ \ldots$, we obtain the values 26, 46, 98, 118, 170, ... which are indeed the higher $\phi/(2\pi)$ values close to which the other minima of Fig. 9 occur.

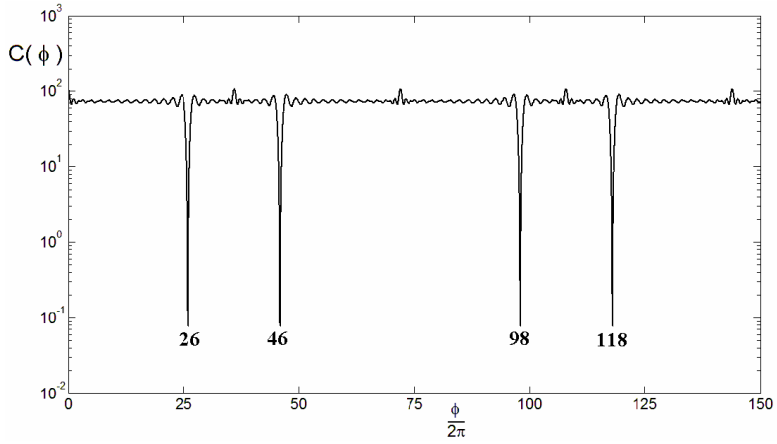

Figure 9. Cost function in logarithmic scale at the odd $m = 26$ resonance of two coupled arrays at a minimum distance $D = 3.0$ ($\lambda_{26}^o = 3.459$).

By focusing on the $\phi \approx 2\pi \times 26$ minimum and by applying a typical function minimization algorithm, we accurately determine the round-trip phase as $\phi(\omega_{odd}) = 2\pi \times 26 + 0.168$. In Fig. 10, we have plotted the continuous function of Eq. (4) for $\phi = \phi(\omega_{odd})$ in comparison with the actual dipole currents computed with the "two-term" theory method. The agreement between the real part of the currents and the standing-wave curve is nearly excellent, while the imaginary part of the currents

is very small as it should be.

Table 1 shows the results for the round-trip phase at the even and odd resonances and their % difference over the resonant value $2\pi \times 26$ of the isolated array, for several minimum distances between the two arrays. As expected, this difference decreases with increasing D.

In order to further investigate the analogy with the coupled optical resonators, some connection between the round-trip phase and the inter-array coupling strength should also be sought for two coupled arrays. A problem arises because the radiative character of coupling between dipoles complicates the task of defining a coupling coefficient between the arrays, in contrast to the well established definition of κ between optical resonators where the coupling is based on the evanescent field ([17] and references therein). To this end, we will here investigate the success of two trial-definitions of inter-array coupling coefficient in predicting the computed round-trip phase split values, and will avoid giving a final explicit definition, which is rather difficult — if not impossible — due to the difference in the coupling mechanism in optical and RF systems.

From the linear system of Eq. (2) follows that the mutual coupling coefficient between elements n and m is $C(n,m) = D(n,m)/D(n,n)$. The simplest definition for an inter-array coupling coefficient would then be to use just the coefficient between the nearest elements of the two arrays, i.e., those at the angles $\theta_1 = \theta_2 = 0^\circ$ (see the Fig. 7

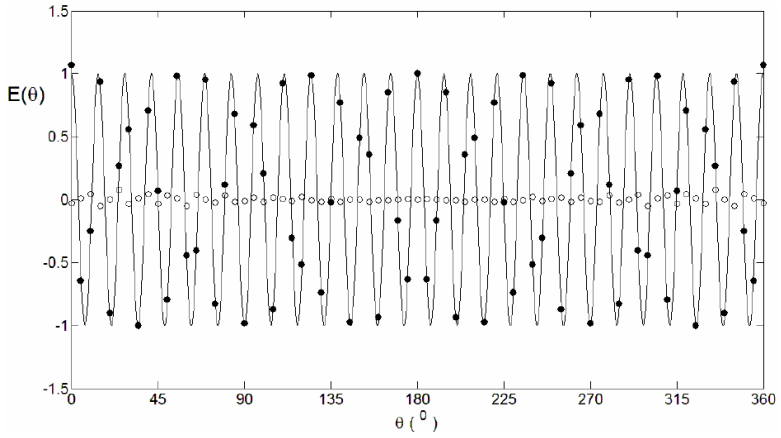

Figure 10. Real (dots) and imaginary (circles) part of dipole currents at the odd $m = 26$ resonance two coupled arrays at a minimum distance $D = 3.0$ ($\lambda^o_{26} = 3.459$) in comparison with Eq. (4) for $\phi(\omega_{odd}) = 2\pi \times 26 + 0.168$.

for the definition of the angles). The result is shown in Fig. 11 in comparison with the above computed round-trip phase differences on even and odd split resonances for several minimum distances between the two arrays. There is some good agreement between the curves for

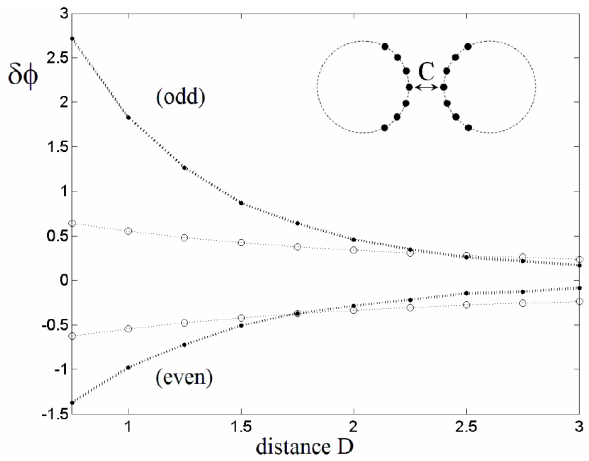

Figure 11. Comparison between the round-trip phase difference $\delta\phi = \phi(\lambda_{26}^{e,o}) - 2\pi \times 26$ of the even and odd $m = 26$ supermode (dots) and the corresponding magnitude (with a negative sign in the even case) of the coupling coefficient between the nearest elements (see the inset) of the two arrays (circles).

Table 1.

D	$\phi(\lambda_{26}^{e})$	$\phi(\lambda_{26}^{o})$	$\delta\phi/\phi(\lambda_{26})(\%)$
0,75	$2\pi \times 26 - 1,373$	$2\pi \times 26 + 2,715$	2,50
1,00	$2\pi \times 26 - 0,979$	$2\pi \times 26 + 1,832$	1,72
1,25	$2\pi \times 26 - 0,722$	$2\pi \times 26 + 1,266$	1,22
1,50	$2\pi \times 26 - 0,509$	$2\pi \times 26 + 0,869$	0,84
1,75	$2\pi \times 26 - 0,373$	$2\pi \times 26 + 0,638$	0,62
2,00	$2\pi \times 26 - 0,285$	$2\pi \times 26 + 0,456$	0,45
2,25	$2\pi \times 26 - 0,217$	$2\pi \times 26 + 0,346$	0,34
2,50	$2\pi \times 26 - 0,148$	$2\pi \times 26 + 0,258$	0,25
2,75	$2\pi \times 26 - 0,129$	$2\pi \times 26 + 0,215$	0,21
3,00	$2\pi \times 26 - 0,087$	$2\pi \times 26 + 0,168$	0,16

minimum distances $D > 2.0$.

A more involved definition of inter-array coupling coefficient is obtained by borrowing the model of an optical variable coupling coefficient coupler [23] which is usually applied to estimate the coupling coefficient between TW optical resonators [17]. According to this model, the mode amplitudes along the interacting region of length L, $A_1(z)$, $A_2(z)$ satisfy two coupled differential equations $dA_1/dz + j\beta \mathrm{A}_1 + j\kappa(z)A_2 = 0$ and $dA_2/dz + j\beta \mathrm{A}_2 + j\kappa(z)A_1 = 0$ where β is the propagation constant and $\kappa(z)$ the variable coupling coefficient. From these equations, follows that the coupling coefficient is equal to the resulting total self- and cross-coupling coefficients are respectively $\tau = \cos(\Phi)$ and $\kappa = \sin(\Phi)$ where $\Phi = \int_L \kappa(z)dz$. By applying this concept in the coupled circular arrays with discrete currents, it is reasonable to define the coupling coefficient at an angle θ_n (see Fig. 7) through the difference $\kappa(\theta_n) = C(\theta_n, \theta_n) - C(\theta_n - \Delta\theta, \theta_n)$ where $\Delta\theta$ is the angular inter-element step. The integral of $\kappa(\theta)$ over the interaction region should then become a discrete sum

$$\Phi = \sum_n \kappa(\theta_n) = \sum_n C(\theta_n, \theta_n) - C(\theta_n - \Delta\theta, \theta_n) \tag{6}$$

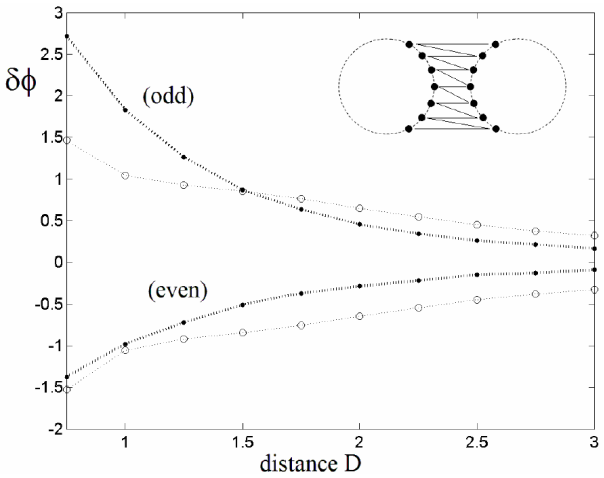

Figure 12. Comparison between the round-trip phase difference $\delta\phi = \phi(\lambda_{26}^{e,o}) - 2\pi \times 26$ of the even and odd $m = 26$ supermode (dots) and the corresponding magnitude (with a negative sign in the even case) of the coupling coefficient $\sin(\Phi)$, with Φ given by Eq. (6) (circles). The inset shows the inter-element coupling coefficients involved in the formula of Eq. (6).

where n covers the elements in the interacting region. Here we have taken into account the elements over the closer semicircles of the two arrays, $|\theta_{1,2}| < 90°$. The result of definition (6) is shown in Fig. 12 in comparison with the computed round-trip phase differences of Table 1. There is clearly some agreement, especially in the case of the odd supermode for minimum distances $D > 1.5$.

4. CONCLUSIONS

This paper has applied the "two-term" method to study the system of two coupled circular loop arrays of dipoles. As expected for any coupled system of wave resonators, the spectral profile of the super-array is characterized by the coupling-induced splitting of the well-studied resonances of the isolated array into symmetric and antisymmetric supermodes with even and odd dipole current distribution along the arrays with respect to the mirror symmetry plane. The circular geometry of these RF cavities brings this system in direct analogy with coupled TW optical cavities, such as WG or microring resonators. By borrowing the standard resonance splitting model from the optical resonator theory, this analogy was numerically investigated and very satisfactory agreement was found between the dipole current distribution in the arrays and the mode profile in TW optical resonators as well as between the dependence of resonance splitting on the coupling strength in the two cases. The reported results are evidence of the underlying connection between the two structures, both being eletromagnetic cavities of circular geometry cavities, stimulating some interest to the direction of incorporating techniques and concepts from the field of optical resonators in order to understand more complex architectures of RF arrays.

REFERENCES

1. Fikioris, G., R. W. P. King, and T. T. Wu, "The resonant circular array of electrically short elements," *J. Appl. Phys.*, Vol. 68, No. 4, 431–439, 1990.
2. Fikioris, G., R. W. P. King, and T. T. Wu, "A novel resonant circular array: Improved analysis," *Progress In Electromagnetics Research*, PIER 8, 1–30, Cambridge, MA, 1994.
3. Fikioris, G., "Experimental study of novel resonant circular arrays," *IEE Proc. Microw. Antennas Propagat.*, Vol. 145, No. 5, 92–98, 1998.

4. King, R. W. P., G. Fikioris, and R. B. Mack, *Cylindrical Antennas and Arrays*, Cambridge University Press, Cambridge, 2002.
5. Fikioris, G., "Resonant arrays of cylindrical dipoles: Theory and experiment," Ph.D. Thesis, Harvard University, 1993.
6. Fikioris, G., R. W. P. King, and T. T. Wu, "Novel surface-wave antenna," *IEE Proc. Microw. Antennas Propagt.*, Vol. 143, No. 1, 1–6, Feb. 1996.
7. Freeman, D. K. and T. T. Wu, "Variational-principle formulation of the two-term theory for arrays of cylindrical dipoles," *IEEE Trans. Antennas Propagat.*, Vol. 43, No. 4, 340–349, Apr. 1995.
8. King, R. W. P., "A microwave beacon and guiding signals for airports and their approaches," *IEEE Trans. Antennas Propagat.*, Vol. 51, No. 1, 110–114, Jan. 2003.
9. Fikioris, G., "Field patterns of resonant noncircular closed-loop arrays," *Journal of Electromagnetic Waves and Applications*, Vol. 10, No. 3, 307–327, 1996.
10. Fikioris, G., S. D. Zaharopoulos, and P. D. Apostolidis, "Field patterns of resonant noncircular closed-loop arrays: Further analysis," *IEEE Trans. Antennas Propagat.*, Vol. 53, No. 12, 3906–3914, Dec. 2005.
11. Fikioris, G., P. J. Papakanellos, J. D. Koundouros, and A. K. Patsiotis, "Difficulties in MoM analyses of resonant circular arrays of cylindrical dipoles," *Electronics Letters*, Vol. 41, No. 2, 54–55, Jan. 20, 2005.
12. Fikioris, G. and K. Matos, "Near fields of resonant circular arrays of cylindrical dipoles," *Antennas and Propagation Magazine, IEEE*, Vol. 50, No. 1, 97–107, Feb. 2008.
13. Rayleigh, L., "The problem of whispering gallery," *Philos. Mag.*, Vol. 20, 1001–1004, Dec. 1910.
14. Vedrenne, C. and J. Arnaud, "Whispering-gallery modes of dielectric resonators," *Proc. Inst. Elect. Eng.*, Vol. 129, No. 4, pt. H, 183–187, Aug. 1982.
15. Matsko, A. B. and V. S. Ilchenko, "Optical resonators with whispering-gallery modes — Part I: Basics," *IEEE J. Select. Topics Quantum Electron.*, Vol. 12, No. 1, 3–14, Jan./Feb. 2006.
16. Ilchenko, V. S. and A. B. Matsko, "Optical resonators with whispering-gallery modes — Part II: Applications," *IEEE J. Select. Topics Quantum Electron.*, Vol. 12, No. 1, 15–32, Jan./Feb. 2006.
17. Little, B. E., S. T. Chu, H. A. Haus, J. Foresi, and J.-P. Laine, "Microring resonator channel dropping filters," *IEEE J. Lightwave*

Technol., Vol. 15, No. 6, 998–1005, June 1997.

18. Smotrova, E. I., A. I. Nosich, T. M. Benson, and P. Sewell, "Optical coupling of whispering-gallery modes of two identical microdisks and its effect on photonic molecule lasing," *IEEE J. Select. Topics Quantum Electron.*, Vol. 12, No. 1, 78–85, Jan./Feb. 2006.
19. Boriskina, S., "Spectrally engineered photonic molecules as optical sensors with enhanced sensitivity: A proposal and numerical analysis," *J. Opt. Soc. Am. B*, Vol. 23, No. 8, 1565–1573, Aug. 2006.
20. Chung, Y., D.-G. Kim, and N. Dagli, "Reflection properties of coupled-ring reflectors," *IEEE J. Lightwave Technol.*, Vol. 24, No. 4, 1865–1874, Apr. 2006.
21. Chremmos, I. D. and N. K. Uzunoglu, "Reflective properties of double-ring resonator system coupled to a waveguide," *IEEE Photon. Technol. Lett.*, Vol. 17, No. 10, 2110–2112, Oct. 2005.
22. Boriskina, S. V., "Coupling of whispering-gallery modes in size-mismatched microdisk photonic molecules," *Opt. Lett.*, Vol. 32, No. 11, 1557–1559, June 2007.
23. Liu, G. J., B. M. Liang, G. L. Jin, and Q. Li, "Switching characteristics of variable coupling coefficient nonlinear directional coupler," *IEEE J. Lightwave Technol.*, Vol. 22, No. 6, 1591–1597, June 2004.